LASER-PLASMA ACCELERATOR BASED EUV-FEL PLASMA SOURCE DEVELOPMENT AT ELI-ERIC*

A. Whitehead† [1,2,3], M. Miceski[1,2,3], S. Maity[4], S. Niekrasz[1,2,3], P. Zimmermann[1,2], P. Sasorov[1,2], A. Jancarek[1,2,3], J. T. Green[1,2], A. Molodozhentsev[1,2]
[1]The Extreme Light Infrastructure ERIC, Dolní Břežany, Czech Republic
[2]ELI Beamlines Facility, Dolní Břežany, Czech Republic
[3]Czech Technical University in Prague, FNSPE, Prague, Czech Republic
[4]Physical Research Laboratory, Atomic, Molecular and Optical Physics Division, Ahmedabad, India

Abstract

Laser-plasma accelerators (LPAs) can generate high-energy, high-quality electron beams, paving the way for a new generation of compact free-electron lasers (FELs). To achieve this, beam stability and repeatability must improve, relying on advances in high-power lasers and plasma-source development. These are key technologies for the 100 Hz LPA-based FEL, under development at ELI ERIC in the frame of the EuPRAXIA project. In this report, we analyse a plasma-target concept designed to generate stable, high-quality electron beams essential for compact Extreme Ultraviolet (EUV) FEL applications. We present a gas filled capillary receiving a high-voltage electrical discharge creating a plasma channels along it. These channels enhance LPA stability by guiding the laser pulse, and maintaining the laser's focus, thereby improving energy transfer. The characteristics of the channel are influenced by the capillary's shape, gas conditions, and discharge setup. Furthermore, we investigate the laser-plasma interaction and electron beam acceleration for the plasma targets using Particle-In-Cell modelling and assess whether the resulting electron beam quality is suitable for LPA-based EUV FEL.

INTRODUCTION

Electron acceleration in plasma-based accelerators (PBAs) can be achieved either with ultra-intense laser pulses, as in laser wakefield acceleration (LWFA) [1], or by using relativistic charged particle beams to drive plasma waves, as in plasma wakefield acceleration (PWFA) [2]. Recent progress within the PBA community has led to improved shot-to-shot stability over long timescales [3, 4] and the production of high-quality electron beams [5], with beam parameters now approaching those required for Free Electron Laser (FEL) applications [6–10]. In parallel, generating electron beams at high repetition rate remains a major focus, particularly with emerging 100 TW-class laser systems operating at 100 Hz [11]. Nonetheless, moving to high-repetition-rate operation introduces two major requirements: the laser must consistently provide ultrashort pulses, and the target must support a plasma source that can operate reliably at the same rate. In this work, the considered plasma target is a gas-filled capillary in which the plasma is generated by a high-voltage pulsed electrical discharge. A three-dimensional magnetohydrodynamic study of hydrogen filling and discharge-plasma formation was previously reported in [12], together with experimental characterisation [13, 14] and a theoretical study of capillary-discharge operation at high repetition rate [15]. In this discharge-driven configuration, the gas is ionised to form a plasma channel that serves as a waveguide for the laser pulse. This preformed channel enables propagation over distances, thereby mitigating diffraction limitations and allowing the use of lower-peak-power laser systems. Plasma targets of this type have already demonstrated the ability to accelerate multi-GeV electron beams [16], and is particularly relevant for extending laser-plasma acceleration to high repetition rates, since lower-peak-power laser systems operating at kilohertz repetition frequencies are already available, and high-repetition-rate capillary discharge waveguides have been demonstrated in [17]. This work contributes to the development of the EUV-FEL at ELI-ERIC [18, 19], driven by the 100 Hz L2-DUHA laser system [11], and for the EuPRAXIA project [20]. The longitudinal plasma density profile was obtained from time-resolved emission spectroscopy using Stark broadening analysis of the hydrogen Balmer-α (Hα) line at 656.3 nm [14]. Three-dimensional particle-in-cell (PIC) simulations, using the experimentally measured plasma density profiles, confirm this target configuration is capable of producing GeV-class electron beams.

PLASMA DISCHARGE CAPILLARY

Experimental Method

The plasma source investigated in this study consists of a 15 mm-long sapphire capillary with a square cross-section of $300 \times 300\,\mu m^2$, filled with hydrogen. The length of the capillary was selected to be less than the dephasing length of the expected electron beam. The experimental method and Stark broadening analysis were described previously in details in [14]. The plasma is produced by a high-voltage electrical discharge applied between electrodes positioned at both ends of the capillary, delivering a current of about 300 A at 25 kV, sufficient to cause rapid electron heating and

* This work was supported by the European Union's Horizon Europe research and innovation programme under grant agreement no. 101079773 (EuPRAXIA Preparatory Phase), no. 101188004 (PACRI–Plasma Accelerator systems for Compact Research Infrastructures), and no. 101073480 and the UKRI guarantee funds (EuPRAXIA Doctoral Network), and by the Ministry of Education, Youth and Sports of the Czech Republic through the e-INFRA CZ, ID:90254.
† alex.whitehead@eli-beams.eu

trigger gas ionisation through collisional processes [21].The plasma emission is collected and coupled into a spectrometer (*Andor Kymera 328i*). The light is dispersed using a 1200 lines/mm diffraction grating and recorded with an intensified scientific Complementary Metal-Oxide-Semiconductor (sCMOS) camera (*Andor iStar*). By introducing an adjustable internal delay, the temporal evolution of the plasma can be resolved. Plasma density is then retrieved using Stark broadening analysis, and the resulting longitudinal density profile is shown in Fig. 1.

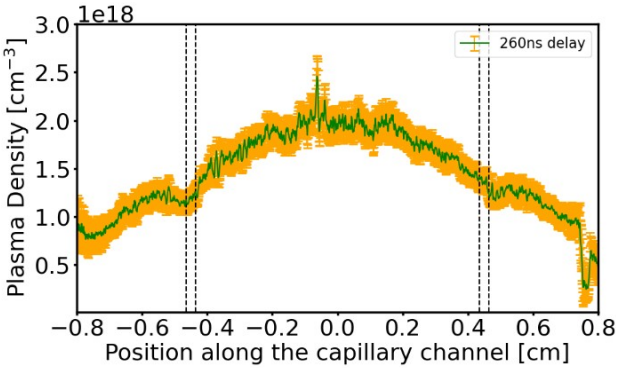

Figure 1: Longitudinal plasma density profiles averaged over 50 images for gas inlet flows of 0.150 mg/s. Discharge parameters: 25 kV voltage, ~300 A current. Dashed black regions indicate gas inlet positions. Top-right values denote camera acquisition delays (10 ns resolution) relative to discharge triggering.

Laser Guiding Structure

During plasma formation, the electron density is higher near the capillary walls than on axis, producing a parabolic plasma channel. The associated radial variation in density modifies the plasma refractive index and enables laser guiding along the capillary axis.In the transverse direction, the electron density profile can be approximated by a parabolic form [21]:

$$n_e(r) \approx n_e(0)\left[1 + 0.33\frac{r^2}{R_{cap}^2}\right], \qquad (1)$$

where R_{cap} is the capillary radius, equal in this work to 150 µm.

A parabolic channel alone is not sufficient to ensure guiding, the laser spot must be properly matched to the plasma channel so that the refractive-index gradient can confine the beam. If the matching condition is not satisfied, the laser will instead undergo self-focusing within the plasma. The matched spot radius is given by [21]:

$$w_m[\mu\text{m}] \approx \frac{1.45\times10^5}{2}\frac{\sqrt{R_{cap}[\mu\text{m}]}}{(n_e[\text{cm}^{-3}])^{1/4}}, \qquad (2)$$

where w_m denotes the matched laser waist.
Assuming an electron density of 1.5×10^{18} cm^{-3}, the corresponding matched laser radius is 26 µm.

PIC SIMULATIONS

Particle-in-cell (PIC) simulations were carried out with the *SMILEI* code [22] in a quasi-3D geometry assuming azimuthal symmetry. The computational domain employed a moving window propagating at the speed of light, with a transverse extent of 100λ resolved with a grid spacing of $\lambda/10$, and a longitudinal length of 80λ resolved with a grid spacing of $\lambda/50$; the time step was set to $\lambda/(51c)$. The driving laser pulse was modelled as a linearly y-polarized Gaussian beam propagating along the x axis. The laser parameters used in the simulations were a central wavelength of 820 nm, an energy of 2 J, and a pulse duration of 30 fs FWHM. The experimentally measured longitudinal plasma density profile, shown in Fig. 1, was used in the simulations, while the transverse density distribution was prescribed by Eq.(1). The simulation results are presented in Fig. 2, 3 and 4. Fig. 2 shows the on-axis plasma density profile extracted from the PIC simulations together with the evolution of the normalized vector potential a_0 as a function of laser propagation distance. Two different laser spot sizes were studied for the same laser energy $w_0 = 20\,\mu$m and 30 µm, with a_0 scaled proportionally to the beam waist in the simulations. For $w_0 = 20\,\mu$m, the laser was initially focused at $x = 8.0$ mm and undergoes self-focusing during propagation. As a result, a_0 increases beyond its vacuum-focus value of about 2.3 and reaches a peak above 4 before decreasing throughout the plasma density profile. In contrast, for $w_0 = 30\,\mu$m with an initial focus at $x = 4.0$ mm, a_0 rises above its vacuum-focus value of about 1.5 and then remains nearly constant across the density plateau, indicating effective laser guiding. These results confirm that operation close to the matching condition is essential, for the present plasma density, the matched radius is approximately 26 µm, which is consistent with guiding for the larger spot size and self-focusing for the smaller one.

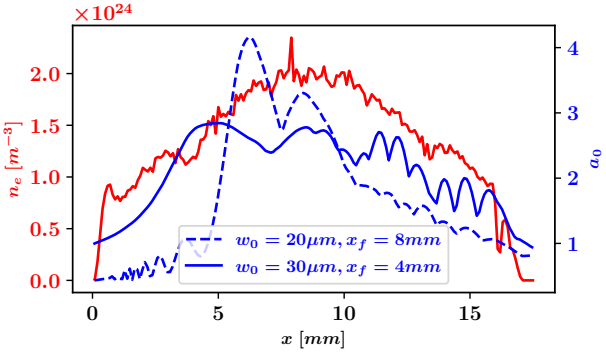

Figure 2: On-axis plasma density n_e (red) and peak normalized vector potential a_0 as a function of laser propagation distance for a laser waist w_0 of 20 μm (solid blue line) and 30 μm. x_f represents the focal position of the laser.

In practice, the laser spot size is typically constrained by the focusing optic upstream of the target. Although the capillary radius R_{cap} could be reduced, this would approach manufacturing limits and impose tighter requirements on laser pointing stability. Alternatively, the plasma density can

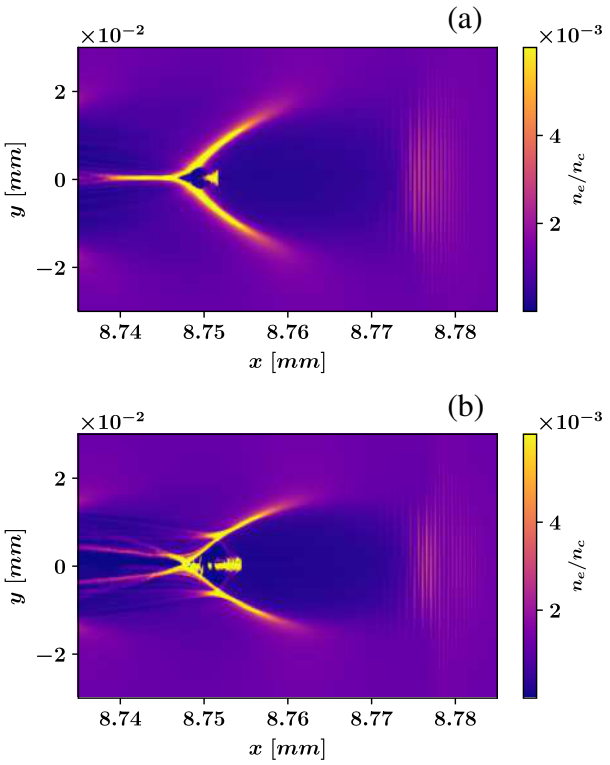

Figure 3: Plasma electron density in the x-y plane at a particular simulation time show electron injection in the first wake structure behind the laser pulse for: (a) w_0 = 30 µm. (b) w_0 = 20 µm.

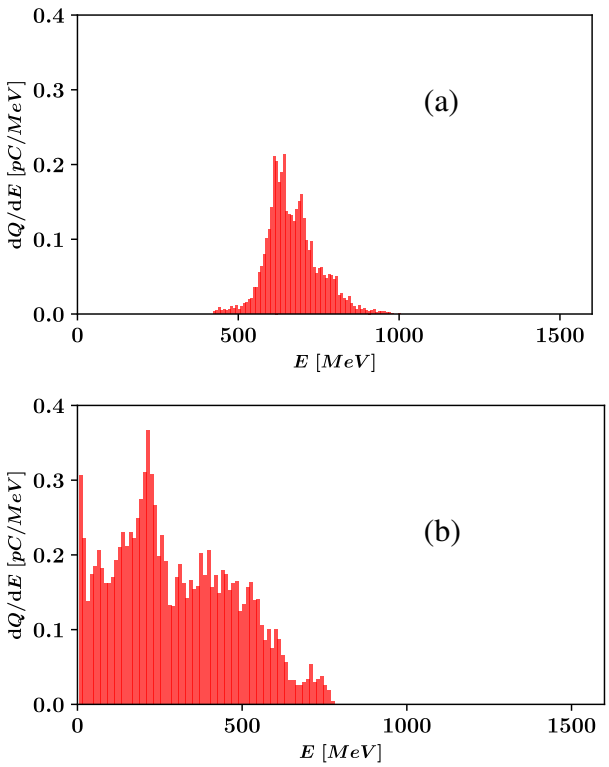

Figure 4: Electron beam energy spectrum at the end of plasma, i.e., x = 17.5 mm for: (a) The guided laser beam with w_0 = 30 µm. (b) The self-focusing laser beam with w_0 = 20 µm.

be increased to achieve a larger matched laser spot size, for the present capillary geometry and w_0 = 20 µm, the required density would be approximately 4 × 10^{18} cm^{-3}, which could be obtained experimentally by raising the gas pressure inside the capillary, and increase accordingly the high-voltage discharge. In both cases, electrons are injected and trapped in the first plasma bubble behind the laser pulse relying on self-injection mechanism and presented in Fig. 3. The results for w_0 = 30 µm and w_0 = 20 µm are presented in Fig. 3(a) and 3(b), respectively. In the guided case, Fig. 4(a) shows that a 15 mm-long discharge capillary driven by a 2.0 J guided laser pulse can produce electron beams with a charge of 30 pC, a mean energy of 670 MeV, and an RMS energy spread of approximately 20 %. The beam has an RMS divergence of about 1.2 mrad horizontally and 1.1 mrad vertically, with corresponding RMS normalized emittances of 1.18 mm-mrad and 1.01 mm-mrad, respectively. By contrast, the non-guided case in Fig. 4(b) yields substantially poorer beam quality, with a charge of 98 pC, a mean energy of 344 MeV, and an RMS energy spread of approximately 162 %. The corresponding RMS divergence increases to 3.2 mrad horizontally and 2.78 mrad vertically, with normalized emittances of 3.68 mm-mrad and 3.07 mm-mrad, respectively.These results highlight the importance of operation in the guided regime, since the longitudinal plasma density profile created by electrical discharge is otherwise insufficiently homogeneous to support the production of high-quality electron beams.

CONCLUSION AND PERSPECTIVES

By using the experimentally measured density profile in PIC simulations we demonstrated an effective acceleration of electron beams in a 15 mm long sapphire capillary, achieving a mean energy of 0.7 GeV in the guided regime. Although the transverse properties of the accelerated electron beams are reasonably good, the energy spread remains high and is therefore incompatible with the requirements for FEL. Meanwhile, in the non-guided regime, the electron beam exhibits poorer beam quality but higher charge, which may be advantageous for applications beyond light sources, such as medical uses. However, by optimising the capillary geometry and tuning the gas parameters, the resulting plasma density profile can be improved, which may enhance the beam quality in both configurations.

REFERENCES

[1] T. Tajima and J. M. Dawson, “Laser electron accelerator”, *Phys. Rev. Lett.*, vol. 43, pp. 267–270, 1979.

[2] P. Chen, J. M. Dawson, R. W. Huff, and T. Katsouleas, “Acceleration of electrons by the interaction of a bunched electron beam with a plasma”, *Phys. Rev. Lett.*, vol. 54, pp. 693–696, 1985. doi:https://doi.org/10.1103/PhysRevLett.54.693

[3] S. Bohlen *et al.*, "Stability of ionization-injection-based laser-plasma accelerators", *Phys. Rev. Accel. Beams*, vol. 25, p. 031301, 2022. doi:https://doi.org/10.1103/PhysRevAccelBeams.25.031301

[4] F. Kohrell *et al.*, "Over 8 hours of continuous operation of a free-electron laser driven by a laser-plasma accelerator", *Phys. Rev. Accel. Beams*, vol. 28, p. 013207, 2026. doi:https://doi.org/10.1103/z2d3-bhyt

[5] W. T. Wang *et al.*, "High-brightness high-energy electron beams from a laser wakefield accelerator via energy chirp control", *Phys. Rev. Lett.*, vol. 117, p. 124801, 2016. doi:https://doi.org/10.1103/PhysRevLett.117.124801

[6] W. Wang *et al.*, "Free-electron lasing at 27 nanometres based on a laser wakefield accelerator", *Nature*, vol. 595, pp. 516–520, 2021. doi:https://doi.org/10.1038/s41586-021-03678-x

[7] R. Pompili, D. Alesini, M. P. Anania, S. Arjmand, M. Behtouei, M. Bellaveglia, *et al.*, "Free-electron lasing with compact beam-driven plasma wakefield accelerator", *Nature*, vol. 605, pp. 659–662, 2022. doi:https://doi.org/10.1038/s41586-022-04589-1

[8] M. Labat *et al.*, "Seeded free-electron laser driven by a compact laser plasma accelerator", *Nat. Photonics*, vol. 17, pp. 150–156, 2023. doi:https://doi.org/10.1038/s41566-022-01104-w

[9] S. K. Barber *et al.*, "Greater than 1000-fold gain in a free-electron laser driven by a laser-plasma accelerator with high reliability", *Phys. Rev. Lett.*, vol. 135, p. 055001, 2025. doi:https://doi.org/10.1103/vh62-gz1p

[10] Z. Jin *et al.*, "Optimized laser wakefield acceleration: generating stable, high-energy, monoenergetic electron beams and demonstrating extreme-ultraviolet free-electron lasers", *Phys. Rev. Research*, vol. 8, p. 013207, 2026. doi:https://doi.org/10.1103/qvg7-ng8n

[11] J. T. Green, R. Antipenkov, P. Bakule, and B. Rus, "L2-duha 100 tw high repetition rate laser system at eli-beamlines. key design considerations", *Rev. Laser Eng.*, vol. 49, pp. 106–109, 2021. doi:https://doi.org/10.2184/lsj.49.2_106

[12] G. A. Bagdasarov, K. O. Kruchinin, A. Y. Molodozhentsev, P. V. Sasorov, S. V. Bulanov, and V. A. Gasilov, "Discharge plasma formation in square capillary with gas supply channels", *Phys. Rev. Res.*, vol. 4, p. 013063, 2022. doi:https://doi.org/10.1103/PhysRevResearch.4.013063

[13] K. O. Kruchinin, A. Mondal, P. V. Sasorov, P. Zimmermann, S. Niekrasz, and A. Y. Molodozhentsev, "Experimental characterization of discharge plasma dynamics in a square capillary for prospective applications in laser wakefield acceleration", *Phys. Plasmas*, vol. 32, p. 043511, 2025. doi:https://doi.org/10.1063/5.0260100

[14] A. Whitehead *et al.*, "Study of electron density in capillary discharge plasma for laser plasma accelerator", *Proc. IPAC*, 2025. doi:10.18429/JACoW-IPAC2025-TUPM097

[15] P. Sasorov, G. Bagdasarov, N. Bobrova, G. Grittani, A. Molodozhentsev, and S. V. Bulanov, "Capillary discharge in the high repetition rate regime", *Phys. Rev. Research*, vol. 6, p. 013290, 2024. doi:https://doi.org/10.1103/PhysRevResearch.6.013290

[16] K. Nakamura *et al.*, "Gev electron beams from a centimeter-scale channel guided laser wakefield accelerator", *Phys. Plasmas*, vol. 14, p. 056708, 2007. doi:https://doi.org/10.1063/1.2718524

[17] A. J. Gonsalves *et al.*, "Demonstration of a high repetition rate capillary discharge waveguide", *J. Appl. Phys.*, vol. 119, p. 033302, 2016. doi:https://doi.org/10.1063/1.4940121

[18] J. K. S. Gupta *et al.*, "Compact undulator-based soft x-ray radiation source at eli", *Proc. SPIE*, vol. 12582, p. 1258209, 2023. doi:https://doi.org/10.1117/12.2665377

[19] M. J. V. D. Let *et al.*, "Plasma accelerator based free electron laser program at eli-eric (eli-beamlines)", in *Proc. 15th Int. Particle Accelerator Conf. (IPAC'24)*, MOPG32, 2024. doi:https://doi.org/10.18429/JACoW-IPAC2024-MOPG32

[20] E. Consortium, "Eupraxia: a compact, multi-gev plasma-based accelerator for user applications", *Eur. Phys. J. Spec. Top.*, vol. 229, pp. 3071–3084, 2020. doi:https://doi.org/10.1140/epjst/e2020-000127-8

[21] N. A. Bobrova *et al.*, "Simulations of a hydrogen-filled capillary discharge waveguide", *Phys. Rev. E*, vol. 65, p. 016407, 2001. doi:https://doi.org/10.1103/PhysRevE.65.016407

[22] J. Derouillat, A. Beck, F. Pérez, T. Vinci, M. Chiaramello, A. Grassi, *et al.*, "Smilei: a collaborative, open-source, multi-purpose particle-in-cell code for plasma simulation", *Comput. Phys. Commun.*, vol. 222, pp. 351–373, 2018. doi:https://doi.org/10.1016/j.cpc.2017.09.024